CMCD: Multipath Detection for Mobile GNSS Receivers

Anton Beitler*, Andreas Tollkühn†, Domenico Giustiniano‡, Bernhard Plattner*
* *ETH Zürich*, † *FAU Erlangen-Nürnberg*, ‡ *IMDEA Networks Institute*

ABSTRACT

In recent years, the rising demand for high precision localization has challenged the use of GNSS particularly in automotive applications. This is especially the case in urban scenarios where the most crucial GNSS disturbance is multipath – the reception of reflected signals. This work addresses the detection of multipath errors in pseudorange measurements for the special case of a moving receiver without the need for redundant observations or motion sensors.

Our proposed detection scheme is based on a combined observable we call *CMCD* (Code-Minus-Carrier Deltarange). It is defined as the difference between code- and carrier-derived deltaranges and approximately resolves to the derivatives of the receiver noise and the code multipath error. The CMCD-based detection algorithm exploits the fact that the CMCD observable is equal to the receiver noise process for multipath-free environments. Simulations of a two ray multipath model show that the code multipath error can be described as a broadband noise process in case of a moving receiver and an abrasive reflection surface. This additional noise process causes changes in the statistical properties of CMCD and hence indicate multipath occurrences. A statistical test is used to detect these changes.

With a test drive under heavy mutlipath conditions the detection performance was evaluated and the suitability of CMCD-based multipath detection was shown. The results indicate a correlation between multipath detections and high ranging errors. In addition, the horizontal position error with a set of 4 satellites was evaluated. In cases of at least one multipath-affected pseudorange a resulting position error of around 15 m (CEP_{95}) and above was observed. With measurements detected as multipath-free the resulting error was around 5 m (CEP_{95}).

INTRODUCTION

A rising demand for very precise and reliable localization in automotive applications can be observed in recent years. Modern advanced driver assistance systems for instance require this precision in order to deliver safety related services, like active collision protection. In open sky scenarios recent low cost GNSS receivers achieve moderate accuracy levels of 5 m (CEP_{95}) and below. However, in urban environments and especially in so-called *urban canyons* (narrow streets with tall buildings) the satellite signals are often blocked or reflected which can lead to errors of more than 10 m (CEP_{95}) due to multipath reception. Till this day, multipath remains the most challenging GNSS error source in terms of detection and mitigation.

In this paper we propose and evaluate a receiver-autonomous code multipath detection scheme suited for mobile receivers in urban navigation. It is based on an observable we define as the *Code-Minus-Carrier Deltarange* or *CMCD* which is the difference between code- and carrier-derived deltaranges, taken from either a single satellite or any satellite pair. This observable allows to distinguish between multipath-free and multipath-affected pseudoranges in real time, solely employing measurements available from off-the-shelf single frequency receivers. CMCD is a generalization of the *successive-time double-difference (STDD)* [1] observable which is restricted to a single satellite. Further, it extends the idea of the known concept of code-minus-carrier (CmC) filtering [2, 3] and applies STDD to the mobile receiver case.

The underlying assumptions are based on a two ray channel model composed of a line-of-sight (LOS) signal path and a single reflected ray as proposed in [3] for this type of channels. It is well known that in the case of a fixed receiver this scenario leads to a pseudorange error component which oscillates well below 1 Hz. We extend this model for kinematic applications by assuming the reflector position to be variant in time mimicking a vehicle's motion in parallel to an uneven wall surface. Simulation results show that if the reflector's horizontal distance of 10 m varies about 10 cm due to surface irregularities the oscillation turns into a broad band noise-like error process as discussed in the *Methods* Section. Hence, the detection of such an additional noise process in the pseudorange measurements would indicate multipath reception.

The CMCD observable allows to isolate this multipath induced code noise from GNSS receiver measurements. An example of a CMCD observation is given in Figure 1. Two distinct regions are characterized by an increased variance and therefore mark the presence of multipath errors in the pseudorange measurement. Hence, our CMCD-based

multipath detection algorithm employs online change-point detection for the variance of subsequent CMCD samples.

For the purpose of evaluating the detection performance and validating the underlying model, we carried out a field campaign in Ingolstadt, Germany. The experimental setup consisted of a low-cost single frequency GPS receiver mounted on a test vehicle as well as an RTK system which served as the reference. The test course was chosen to include the narrow alleys of Ingolstadt city where multipath reception was highly probable. The results show that in cases where our algorithm indicated a multipath-affected environment the ranging errors were as high as 15 m (Q_{95}) while in the alternative case ranging errors in the order of 2.5 m (Q_{95}) were observed.

Related Work

The problem of multipath reception in GNSS receivers has been addressed in numerous publications. Aside from the standard GNSS literature such as [4] and [5], comprehensive coverage of multipath aspects is provided in [2]. The way in which multipath affects specific measurements in the GNSS receiver has been analyzed in great detail by [6]. The awareness of multipath being the most severe error source led to an abundance of detection and mitigation proposals in numerous papers. [3] provides an excellent overview of the most striking approaches with particular focus on signal processing techniques.

The realm of algorithmic approaches based on GNSS receiver measurements can be grouped into filtering methods and snapshot methods depending on whether or not past measurements are considered in the heuristic. The most dominant snapshot algorithm is *Snapshot RAIM* [7] and multiple derivatives thereof, like [8, 9]. These share the common approach to model a multipath affected measurement as an outlier in the measurement set and to infer the integrity of measurements through mutual comparison of their residuals. Filtering methods often employ dynamic models to predict the receiver's position and use it as a measure of integrity [10, 11]. Such approaches are referred to as *Sequential RAIM*.

Other methods model multipath as a time varying error and detect such changes in the measurements. For example, in the case of fixed receivers, multipath errors oscillate at low frequencies [2]. This characteristic can be detected and mitigated by frequency domain analyses [12]. Moreover, it has been shown that these oscillations are recurring on a daily basis. Therefore, recorded observations can be used to predict the multipath error of the following day [13]. Yet another approach detects variance changes in the GNSS observations that are related to multipath [14]. In [1] the dual-epoch observable is introduced and bounds for the minimum detecable jumps and ramps are derived.

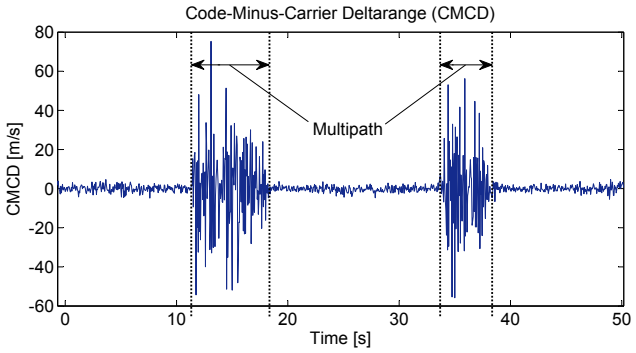

Figure 1. Example of a CMCD measurement over a time period of 100 s. Two regions show an increased variance which indicates multipath reception.

Contribution

This work extends the multipath error models as in [2] and [3] to a dynamic multipath model similar to [1] which applies for a mobile receiver in an urban environment. Based on these models a combined observable which allows to isolate the code multipath process has been applied. These findings were incorporated in the development of a real time multipath detection method that works independently from external data and is robust to common mode errors. Finally, we evaluated the proposed method in a real world experiment and demonstrated its suitability.

Outline

In the *Methods* Section the multipath signal model of the two-ray case is introduced and its impact shown on the code tracking loops of a receiver. Further, an overview of the GNSS observables is given as well as their model's derivations which are relevant to this work. The *Deltarange-based GNSS Multipath Detection* Section constitutes the core of this paper explaining our detection approach in detail including the derivation and a statistical description of the CMCD observable. A mathematical description of the detection algorithm is presented in this section as well. The *Experimental Setup* Section lays out the tools and methods used during the evaluation campaign which was carried out with the purpose to evaluate the algorithm's performance and to validate the underlying proposed models. The results are summarized in the *Evaluation* Section including four evaluation procedures, namely a visual inspection of the camera data, a statistical evaluation of the CMCD observable under LOS conditions, and finally an error-based performance evaluation in the position domain and in the measurement domain.

METHODS

Multipath propagation is a common phenomenon in radio communication and radio navigation and occurs whenever a received electromagnetic wave has traveled on a path other than the direct line of sight between the transmitting and receiving antennas. The detection of multipath requires a model for the characteristics of a multipath affected received signal. What follows is a description of such a model which characterizes multipath errors in mobile GNSS receivers as additional noise in the pseudorange measurements.

Single Reflected Ray Channel Model

For the purpose of this work a *single reflected ray* channel model is employed which consists of two propagation paths: the line of sight from the satellite to the receiver as well as one single reflection.

In this scenario the received multipath-affected signal $s_M(t)$ for a single satellite is a superposition of the direct signal and and its delayed and attenuated copy. Thus, the compound signal can be expressed as

$$s_M(t) = A_0 \cdot C(t)\cos(\omega_0 t) + A_M \cdot C(t-\tau_M)\cos(\omega_0 t + \phi_M) \quad (1)$$

where $C(t)$ denotes the amplitude modulated spreading code sequence. In addition to the amplitude A_0 and the carrier frequency w_0 the signal is characterized by three multipath parameters. First, the *multipath amplitude* A_M which is related to the direct signal amplitude by $\alpha_M = A_M/A_0$. Second, the *multipath delay* τ_M which is the time shift between the direct signal and the multipath signal. This quantity can either be expressed in terms of time or geometric lengths. Third, the *multipath relative phase* ϕ_M quantifying the phase shift between the multipath signal and the direct signal which results from the path delay.

Code Multipath Model for Mobile Receivers

A simple type of code tracking loops employ early-minus-late discriminators. Such tracking loops correlate the received signal with two delayed code sequence replicas, the early and late code. Thereby, the two replicas have a fixed mutual delay of d chip widths (d is referred to as the *correlator spacing*) and a common variable delay of $\hat{\tau}$ with respect to the incoming signal. The normalized multipath-free early-minus-late discriminator function is given by

$$D(\hat{\tau}) = R\left(\hat{\tau} + \frac{T_C \cdot d}{2}\right) - R\left(\hat{\tau} - \frac{T_C \cdot d}{2}\right) \quad (2)$$

with T_C denoting the chip width and $R(\tau)$ the triangle-shaped autocorrelation function of the spreading sequence. The goal of the tracking loop is to achieve a phase lock with the incoming signal by adjusting $\hat{\tau}$ in such a way that $D(\hat{\tau})$ is zero. The amount by which $\hat{\tau}$ is adjusted gives rise to the range measurement between the satellite and the receiving antenna.

Under multipath conditions, however, the additional shifted signal copies cause a skewed and asymmetric autocorrelation function of the compound signal. As a result, the tracking loop fails to lock to the direct signal and the range measurement is distorted.

Considering the multipath reception model of Equation 1, the resulting multipath-affected discriminator function $D_M(\hat{\tau})$ comprises a superposition of the multipath-free discriminator function as well as a shifted and attenuated copy:

$$D_M(\hat{\tau}) = D(\hat{\tau}) + \alpha_M \cdot D(\hat{\tau} - \tau_M) \cdot \cos(\phi_M). \quad (3)$$

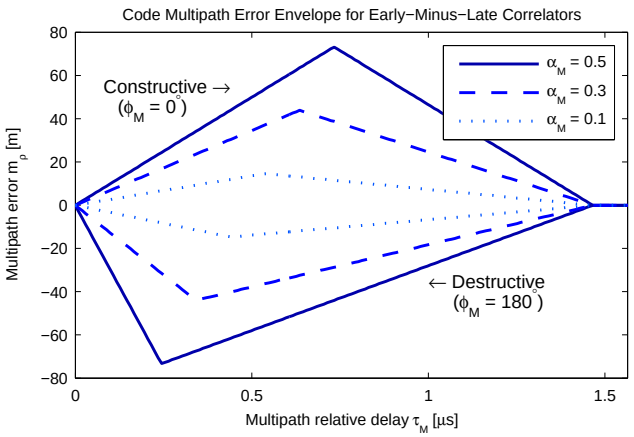

Figure 2. Code multipath error envelope for early-minus-late correlators ($d = 1$) as a function of the multipath delay τ_M. The envelope forms the bounds for possible multipath errors.

The multipath-induced error m_ρ on the code-derived range measurements corresponds to the zero crossing of this discriminator function. A graph of the multipath error bounds for given relative delays τ_M results in what is known as the *code multipath error envelope*. Figure 2 shows the error envelope for early-minus-late correlators with spacing $d = 1$ for the relative multipath amplitudes $\alpha_M = \{0.5, 0.3, 0.1\}$. For arbitrary multipath relative phases ϕ_m the error lies inside the envelope. In the case of the single reflected ray model, the envelope constitutes the ranging error for the border cases of constructive ($\phi_M = 0°$) and destructive interference ($\phi_M = 180°$).

In order to analyze the code multipath error for mobile receivers we have to consider its behavior over time. Equation 3 indicates that this is mainly governed by the time varying multipath relative phase $\phi_M(t)$. For a qualitative analysis of this quantity we employ the single reflected ray model [3, Section 3]. Its graphical depiction is given in Figure 3. This model allows to express $\phi_M(t)$ as a function of the receiver's surrounding geometry, namely the satellite's azimuth $A^S(t)$ and elevation $E^S(t)$ as well as the reflector's position expressed in azimuth A_R, elevation E_R,

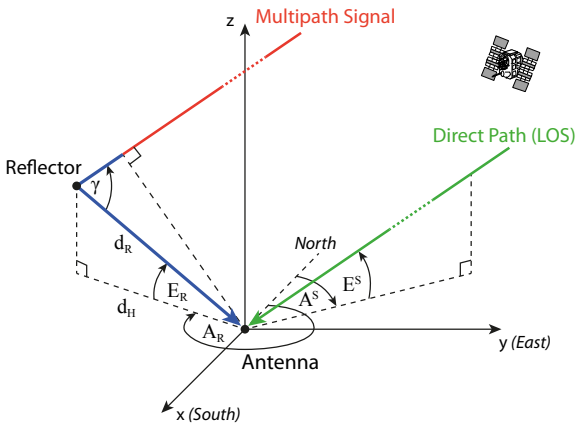

Figure 3. Single reflected ray model. Source: [3, Figure 3-9]

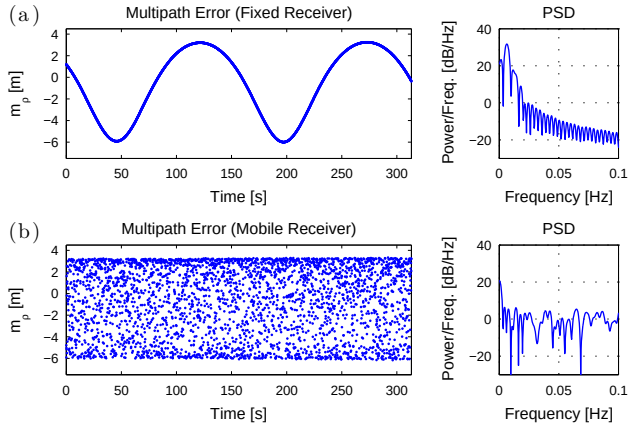

Figure 4. Multipath induced range error oscillation in the fixed and mobile receiver case. (a) In the fixed case a clear sinusoidal error evolves. (b) In the mobile case no distinct frequency is visible.

and horizontal distance d_H [3, Eqn. 21]:

$$\phi_M(t) = \frac{2\pi}{\lambda}\frac{d_H}{\cos E_R} \cdot \cdot \left(1 - \cos E^S(t)\cos E_R \cos\left(A^S(t) - A_R\right) - \sin E^S(t)\sin E_R\right). \quad (4)$$

The temporal evolution of $\phi_M(t)$ in the case of a fixed reflector ($\{A_R, E_R, d_H\} = \text{const.}$) is solely induced by the changing satellite position $(A^S(t), E^S(t))$. Figure 4(a) shows the behavior of the range error m_ρ under such conditions which results in a sinusoidal oscillation. For this example a real satellite trajectory was used and a fixed horizontal reflector distance of $d_H = 10$ m was selected. The frequency of the multipath error is proportional to the distance d between the reflector and the receiver.

The application of this analysis on a vehicle navigation scenario in an urban canyon requires a mobile receiver model. This can be achieved by introduction of a time-varying horizontal reflector distance d_H as it simulates a receiver movement in parallel to a coarsely textured wall surface. In Figure 4(b) d_H has been set to $d_H = 10 + \epsilon$ m where $\epsilon \sim \mathcal{N}(0, 0.1^2)$ is a Gaussian noise process with a chosen standard deviation of 10 cm. As a consequence, the distinct frequency in the multipath error vanishes and its power spectral density becomes nearly constant. Hence, the code multipath error in mobile receivers can be described as a noise process.

GNSS Observables and their Measurement Models

Apart from the multipath induced errors in the code tracking loops, many other error sources have to be taken into account. The following is an overview of the error models for the common GNSS observables. These models later serve as the basis for the new combined observable CMCD.

The two elementary range measurements obtained in a typical receiver are the code delay and Doppler shift of a channel. From these two "raw" measurements a number of derived observables can be formed. The *pseudorange* observable is formed from code delay measurements and the *carrier phase* observable is derived from the Doppler measurement. The *deltarange* observable can be formed in both, the code- and the carrier domain. Table 1 summarizes these observables and their units of measure.

Table 1. Raw and derived observables from GNSS receivers.

Domain	Observable	Symbol	Unit
Raw Observables			
Carrier	Doppler shift	–	[Hz]
Code	Code delay	–	[s]
Derived Observables			
Code	Pseudorange	$\rho^{(k)}$	[m]
Carrier	Carrier phase	$\phi^{(k)}$	[L1 cycles]
Carrier/Code	Deltarange	$D^{(k)}$	[m/s]

Pseudorange $\rho^{(k)}$ A pseudorange is a range measurement which differs from the true geometric range $r^{(k)}$ due to a number of error sources. The class of *common mode errors* result from sources that have equal impact on all receivers within a certain proximity. These include the satellite clock errors $\delta t^{(k)}$ as well as atmospheric effects like the ionospheric group delay $I^{(k)}$ and tropospheric group delay $T^{(k)}$. The common mode errors tend to change slowly over time. Additional error sources include receiver clock errors δt_u and code multipath reception $\alpha m_\rho^{(k)}$.

The resulting pseudorange measurement model can be expressed as

$$\rho^{(k)} = r^{(k)} + c\left[\delta t_u - \delta t^{(k)}\right] + I^{(k)} + T^{(k)} + \alpha m_\rho^{(k)} + \varepsilon_\rho^{(k)} \quad (5)$$

where α is a binary code multipath indicator variable. The additive code measurement noise term $\varepsilon_\rho^{(k)}$ confines the residual error processes such as thermal noise and diffuse reflections and can be modeled as uncorrelated, zero-mean, Gaussian distributed noise.

Carrier Phase $\phi^{(k)}$ The carrier phase observable is a running count of the number of carrier cycles between the receiver and the satellite position. It is typically expressed in the number of carrier wavelengths λ.

The measurement model of the carrier phase [5, Eqn. 5.47]

$$\lambda\phi^{(k)} = r^{(k)} + c\left[\delta t_u - \delta t^{(k)}\right] - I^{(k)} + T^{(k)} + \lambda N^{(k)} + \alpha m_\phi^{(k)} + \varepsilon_\phi^{(k)} \quad (6)$$

shares similarities with Equation 5 because it is a range measurement, as well. However, the main difference is the additional ambiguity term $\lambda N^{(k)}$ which accounts for the unknown initial cycle count. Furthermore, the dispersion of the ionosphere causes a phase advance as opposed to a delay which accounts for the negative sign of the ionospheric

error term [5, Eqn. 5.25]. The carrier phase multipath error $\alpha m_\phi^{(k)}$ and the carrier phase measurement noise $\varepsilon_\phi^{(k)}$ are analogous to their code domain counterparts of Equation 5. However, in comparison, their amplitude is negligibly small [5, Table 5.2].

Deltarange $D^{(k)}$ The deltarange measurement is the rate of change in the distance between the receiver and a satellite, i.e. the relative speed in line of sight direction and is therefore directly related to the Doppler frequency. The deltarange observable can be obtained through the pseudorange and the carrier phase observables, namely by differencing consecutive range measurements.

The code-derived deltarange observable $D_\rho^{(k)}$ yields

$$\begin{aligned} D_\rho^{(k)} &= \dot{\rho}^{(k)}(t) \\ &= \dot{r}^{(k)} + c[\delta\dot{t}_u - \delta\dot{t}^{(k)}] + \dot{I}^{(k)} + \dot{T}^{(k)} + \alpha\dot{m}_\rho^{(k)} + \dot{\varepsilon}_\rho^{(k)} \\ &\approx \dot{r}^{(k)} + c\delta\dot{t}_u + \alpha\dot{m}_\rho^{(k)} + \dot{\varepsilon}_\rho^{(k)}. \end{aligned} \tag{7}$$

where the dot indicates the time derivative. The approximation assumes that $I^{(k)}$, $T^{(k)}$ and $\delta t^{(k)}$ change very slowly over time such that their time derivatives are very small compared to the multipath error.

For the carrier-derived deltarange observable $D_\phi^{(k)}$ one obtains similarly

$$\begin{aligned} D_\phi^{(k)} &= \lambda\dot{\phi}^{(k)}(t) \\ &= \dot{r}^{(k)} + c[\delta\dot{t}_u - \delta\dot{t}^{(k)}] \\ &\quad - \dot{I}^{(k)} + \dot{T}^{(k)} + \lambda\dot{N}^{(k)} + \alpha\dot{m}_\phi^{(k)} + \dot{\varepsilon}_\phi^{(k)} \\ &\approx \dot{r}^{(k)} + c\delta\dot{t}_u + \alpha\dot{m}_\phi^{(k)} + \dot{\varepsilon}_\phi^{(k)} \end{aligned} \tag{8}$$

applying the previous approximations. Additionally, the assumption of a constant ambiguity term $\lambda N^{(k)}$ is implied which assumes the absence of cycle slips.

DELTARANGE-BASED MULTIPATH DETECTION

The Code-Minus-Carrier Deltarange

The *Code-minus-Carrier Deltarange* (CMCD) observable applies the concept of CmC [2, 3] on the deltarange level. The special case of using the observables from each satellite separately was proposed in a similar context as *STDD* [1]. Its goal is to isolate the code multipath error without the use of external information. CMCD achieves this by taking the difference between the code-derived and carrier-derived deltarange observables. These can, in principle, originate from different satellites. The definition of CMCD for a given satellite pair (k, l) therefore yields

$$CMCD = D_\rho^{(k)} - D_\phi^{(l)} = \dot{\rho}^{(k)} - \lambda\dot{\phi}^{(l)}. \tag{9}$$

The application of the measurement models from Equations 7 and 8 leads to

$$\begin{aligned} CMCD &= \dot{\rho}^{(k)} - \lambda\dot{\phi}^{(l)} \\ &\approx \left(\dot{r}^{(k)} + \cancel{c\delta\dot{t}_u} + \alpha\dot{m}_\rho^{(k)} + \dot{\varepsilon}_\rho^{(k)}\right) \\ &\quad - \left(\dot{r}^{(l)} + \cancel{c\delta\dot{t}_u} + \cancel{\alpha\dot{m}_\phi^{(l)}} + \cancel{\dot{\varepsilon}_\phi^{(l)}}\right) \\ &\approx \left(\dot{r}^{(k)} - \dot{r}^{(l)}\right) + \alpha\dot{m}_\rho^{(k)} + \dot{\varepsilon}_\rho^{(k)} \end{aligned} \tag{10}$$

which shows that the receiver clock drifts cancel out. Additionally, the negligible magnitude of the carrier phase multipath and carrier measurement noise processes can be disregarded. This results in a superposition of a geometric term and two additive noise processes. In practice, the geometric term can be predicted from the satellites' and receiver's motions.

An alternative formulation of CMCD without the need for dynamic prediction is given for the case where code- and carrier derived deltarange observations are taken from the same satellite ($k = l$). In this case the geometry term drops and the CMCD observable yields

$$CMCD = \dot{\rho}^{(k)} - \lambda\dot{\phi}^{(k)} \approx \alpha\dot{m}_\rho^{(k)} + \dot{\varepsilon}_\rho^{(k)}. \tag{11}$$

This corresponds to the time derivative of the CmC observable, taking into account the approximations mentioned before. Due to its simplicity, the CMCD formulation of Equation 11 is particularly favorable. However, certain situations may justify the use of Equation 10, for example in cases where the carrier derived measurement is known to be corrupted.

A possible CMCD observation has already been shown in Figure 1. Five distinct time periods can be distinguished there. Three of them contain a low power noise process, the other two contain a higher power noise process. The high power noise processes are multipath induced code delay errors under mobile receiver conditions. The low power noise is the residual receiver noise process $\dot{\varepsilon}_\rho^{(k)}$.

Statistical Properties of CMCD

The key to detecting multipath with the help of CMCD lies in its statistical properties. As the example has shown, a change in the variance of CMCD is what indicates multipath presence. In order to detect this change, its variance without multipath has to be known.

The definition of CMCD in Equation 11 implies that under no-multipath conditions ($\alpha = 0$), CMCD equals the time derivative of the receiver noise which is modeled as a white Gaussian noise process with zero-mean and a characteristic variance σ_0^2.

For the analysis of the discrete probability distribution of a set of CMCD measurements under no-multipath conditions, consider the random vector $\boldsymbol{\varepsilon}$ whose elements are n independent observations of the receiver noise $\varepsilon_\rho(t)$ at distinct time instances $t_1, t_2, \ldots, t_n$:

$$\boldsymbol{\varepsilon} = (\varepsilon_\rho(t_1), \varepsilon_\rho(t_2), \ldots, \varepsilon_\rho(t_n)) \tag{12}$$

This random vector follows a multivariate Gaussian distribution with mean vector $\boldsymbol{\mu} = 0$ and covariance matrix $\boldsymbol{\Sigma} = \sigma_0^2 \boldsymbol{I}$, with $\boldsymbol{I}$ being the identity matrix. The discrete time derivative of $\boldsymbol{\varepsilon}$ can be approximated by a backward difference which corresponds to a multiplication with a matrix

$$\boldsymbol{D} = \begin{bmatrix} -1 & 1 & & \\ & \ddots & \ddots & \\ & & -1 & 1 \end{bmatrix} \tag{13}$$

assuming a sampling rate of 1 Hz. This operation results in an $n-1$ dimensional random vector

$$\begin{aligned} \tilde{\boldsymbol{\varepsilon}} &= \boldsymbol{D}\boldsymbol{\varepsilon} \\ &= (\varepsilon_\rho(t_2) - \varepsilon_\rho(t_1), \ldots, \varepsilon_\rho(t_n) - \varepsilon_\rho(t_{n-1})) \end{aligned} \tag{14}$$

which is Gaussian distributed with zero-mean and covariance matrix

$$\tilde{\boldsymbol{\Sigma}} = \boldsymbol{D}\boldsymbol{\Sigma}\boldsymbol{D}^\top = \begin{bmatrix} 2\sigma_0^2 & -\sigma_0^2 & & & \\ -\sigma_0^2 & 2\sigma_0^2 & \ddots & & \\ & \ddots & \ddots & \ddots & \\ & & \ddots & 2\sigma_0^2 & -\sigma_0^2 \\ & & & -\sigma_0^2 & 2\sigma_0^2 \end{bmatrix}. \tag{15}$$

In a multipath scenario an additive noise process changes the statistical properties of the CMCD observable. Without further specification of the multipath process' statistical properties it can be assumed that under multipath the variance of the CMCD observation increases because the receiver noise and the multipath process are uncorrelated.

CMCD-based Multipath Detection

The detection of multipath corrupted range measurements in a mobile receiver based on CMCD relies on its changing statistical properties depending on whether or not multipath reception is present. The approach described hereafter is a changepoint detection algorithm for the variance.

For a data vector $\mathbf{x}$ containing the last w CMCD observations at time step k, a sample variance estimate is given by

$$s_k^2 = \frac{\mathbf{x}^\top \mathbf{x}}{w}. \tag{16}$$

This gives rise to the hypotheses for a statistical test:

$$\begin{aligned} H_0 &: s_k^2 = 2\sigma_0^2 \qquad \text{“No multipath at time } k\text{.”} \\ H_1 &: s_k^2 > 2\sigma_0^2 \qquad \text{“Multipath present at time } k\text{.”} \end{aligned}$$

where σ_0^2 is the known characteristic receiver noise variance. The following statistic T_k is used for a single-tailed significance test:

$$T_k = w \cdot \frac{s_k^2}{2\sigma_0^2}. \tag{17}$$

Table 2. List of critical values $t_{\alpha,w}$

w	$t_{0.02,w}$	$t_{0.05,w}$	w	$t_{0.02,w}$	$t_{0.05,w}$
1	–	–	11	25.72	21.71
2	8.76	6.42	12	27.28	23.16
3	11.27	8.58	13	28.82	24.59
4	13.46	10.51	14	30.33	26.00
5	15.46	12.30	15	31.82	27.39
6	17.33	14.00	16	33.29	28.77
7	19.12	15.62	17	34.75	30.14
8	20.84	17.20	18	36.19	31.50
9	22.51	18.74	19	37.62	32.84
10	24.13	20.24	20	39.04	34.18

This is a suitable test statistic because its distribution under the null-hypothesis is known. For a given significance level α the decision rule is a comparison with the critical value $t_{\alpha,w}$ of the particular distribution:

$$T_k > t_{\alpha,w} \implies \text{Reject } H_0 \tag{18}$$

Under the null-hypothesis the test statistic T_k is a quadratic form of a Gaussian distributed random vector $\mathbf{x}$ with correlated elements, thus $\mathbf{x} \sim \mathcal{N}(0, \tilde{\boldsymbol{\Sigma}})$. For its probability distribution several representations in form of series expansions exist [15, Ch. 4]. However, for an efficient implementation of the detection algorithm a lookup-table of critical values for given significance levels α and window sizes w is supplied in Table 2.

EXPERIMENTAL SETUP

During two measurement campaigns a large data basis was acquired for use in offline analyses. The measurement equipment which was mounted on a vehicle included a ublox7 GPS receiver running at a rate of 10 Hz, an iMar iTrace F400 reference measurement unit, a camera, and data recording and storage devices. The GPS receiver provided code- and carrier based range measurements as well as timing and satellite position information. The reference system provided precise position and heading information. The camera only served as a visual reference for signal obstruction. It was mounted on the roof of the vehicle in proximity to the GPS antenna.

Correction Data Processing

In order to focus on the evaluation of the multipath error further errors, and in particular the common-mode error, had to be accounted for. The error correction post processing included the following steps.

For the correction of the satellite clock the polynomial clock bias and drift model was used. The parameters were obtained from the navigation message. The ionospheric error was corrected with the help of a TEC map available at the International GNSS Service (IGS) web page. For compensating the tropospheric errors, zenith path delay measurements were obtained from IGS, as well. In particular the zenith path delay measurements from the

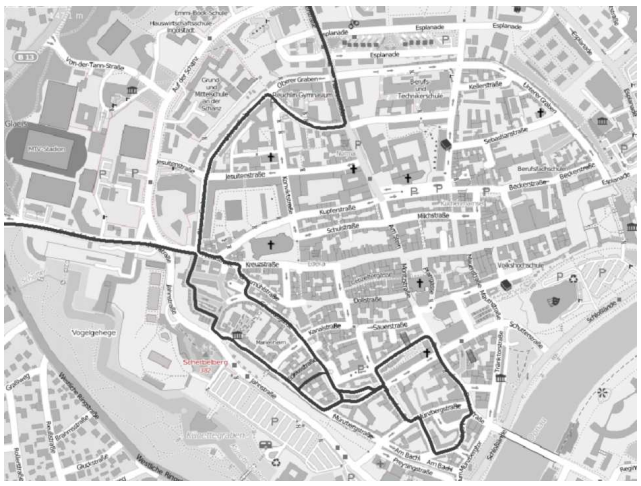

Figure 5. The chosen track for Measurement Campaign 1 on December 18th, 2013. (© OpenStreetMap contributors)

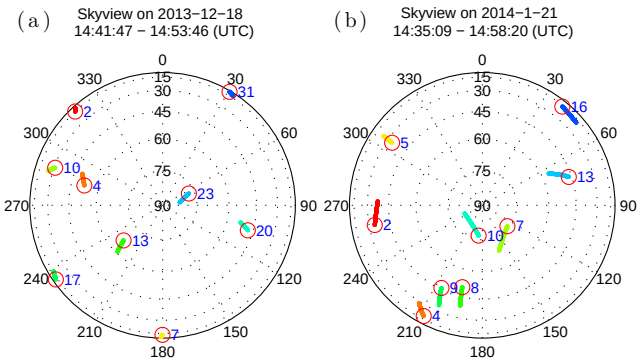

Figure 6. Skyview during the two measurement periods (a) on December 18, 2013, 14:41:47 – 14:53:46 UTC; (b) on January 21, 2014, 14:35:09– 14:58:20 UTC.

reference station in Bad Koetzting, Germany located at 12.8789° N, 49.1442° E were used.

Measurement Campaign 1: Mobile Receiver, Urban Areas

One measurement campaign has been conducted in Ingolstadt, Germany on December 18, 2013 between 14:41:47 and 14:53:46 (UTC) in order to assess the suitability and quality of CMCD-based multipath detection in urban environments. The track has been chosen to contain severely obstructed vision to the sky which is typical for urban canyons. Figure 5 is a map of the chosen track through the old town's narrow streets. Figure 6(a) shows the constellation of satellites during the measurement period.

Measurement Campaign 2: Fixed Receiver, no Multipath

For a statistical evaluation of the CMCD observable under no-multipath conditions a measurement with a fixed receiver has been carried out on January 21, 2014 between 14:35:09 and 14:58:20 (UTC). The reference position of the receiver was (48.812403°, 11.354697°, 438.95 m) expressed in LLH (HAE) coordinates. Figure 6(b) shows the skyview of the satellites during the measurement period.

The goal of this measurement campaign was to validate the statistical model of CMCD without multipath reception,

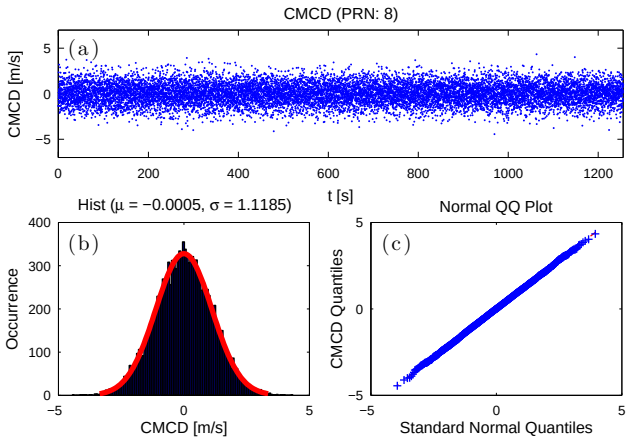

Figure 7. The statistical properties of the CMCD Observable of Satellite 8 at no multipath.

which was assumed to be zero mean and Gaussian distributed. For that purpose 12553 data samples of the code and carrier observable of each satellite in view have been recorded at a rate of 10 Hz.

EVALUATION

The data obtained from the measurement campaigns was used to prove the assumptions on CMCD's statistical properties and for a three step evaluation of CMCD-based multipath detection. First, a visual inspection was carried out based on the camera data and the detection results. Second, the detection algorithm was evaluated in the measurement domain. And finally, an evaluation in the position domain was performed.

Statistical Evaluation of CMCD

From the set of 12553 data samples recorded at the field campaign on January 21, 2014, the CMCD observable was obtained. For each satellite a normal fit on the histogram of the data set has been done. A χ^2 goodness of fit test with significance level $\alpha = 0.05$ was used to assess whether the distribution of the data was Gaussian.

Figure 7 shows the statistical evaluation data set on the example of Satellite 8. In Figure 7(a) the CMCD observation over the measurement period of about 20 minutes is given. Figure 7(b) shows the histogram with a fitted normal distribution with parameters $\mu = -0.0005$ and $\sigma = 1.1185$. The goodness of fit test did not reject the null-hypothesis of the data being Gaussian. Figure 7(c) shows the QQ-plot of the data. The ordinate is scaled in such a way that a cumulative normal distribution function results in a line. It can be seen that the data perfectly aligns in a straight line.

The fixed receiver measurement indicates that CMCD is indeed Gaussian distributed in a no-multipath environment. The mean value is in the order of millimeters and the standard deviation is between $\sqrt{1.07}$ m and $\sqrt{1.12}$ m. The assumptions of a stationary, zero-mean Gaussian process can therefore be affirmed.

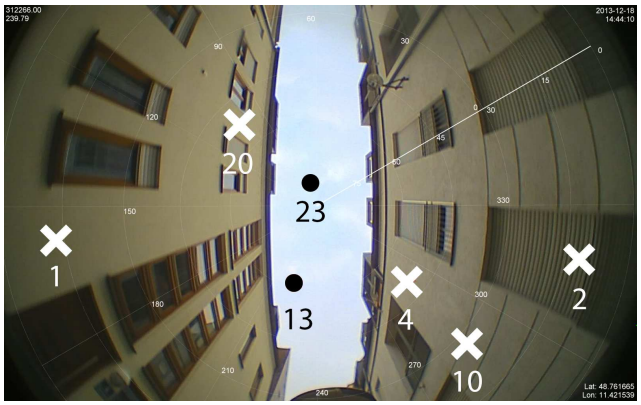

Figure 8. Impression from inside an urban canyon.

Visual Inspection

Figure 8 shows an instance from the Ingolstadt City trajectory captured by the camera. The satellite positions are projected into the image to represent the LOS directions. The satellite positions are indicated as dots when no multipath reception was detected. Crosses are used when a detection by the multipath detector occurred.

The behavior of the detection algorithm in this instance was as expected. The received signals to which the LOS was blocked had to be a reflection and a multipath detection had to occur. This was true for Satellites 1, 2, 4, 10 and 20. Satellites to which a clear sight existed did not necessarily have to be affected by multipath.

Measurement Domain Evaluation

From the reference receiver data and the corrected satellite positions the true geometric range $r^{(k)}$ can be obtained. Assuming perfectly corrected common-mode errors the isolated error for the pseudorange model of Equation 5 resolves to

$$\mathcal{E}^{(k)} = \rho^{(k)} - r^{(k)} \approx c\delta t_u + \alpha m_\rho^{(k)} + \varepsilon_\rho^{(k)}. \qquad (19)$$

However, the receiver clock δt_u, the dominating error term, cannot be modeled due to its instability and renders a multipath error analysis useless. The receiver clock error estimate $\delta\hat{t}_u$ obtained from a least squares position solver cannot be used for compensation because it bears the same error, only transformed into the solution domain. This would severely degrade the error analysis.

In order to address this problem, we use the *single difference error* SD_e as the error evaluation metric. The single difference is defined as the difference between the pseudorange observations of a the satellite in question $\rho^{(k)}$ and a reference satellite $\rho^{(\mathrm{ref})}$. Hence, the single difference error is an approximation of the multipath induced error in the pseudorange measurement. It is given by

$$SD_{\mathrm{e}}^{(k)} = \mathcal{E}^{(k)} - \mathcal{E}^{(\mathrm{ref})} \approx \alpha m_\rho^{(k)} + \varepsilon_\rho^{(k)} - \varepsilon_\rho^{(\mathrm{ref})} \qquad (20)$$

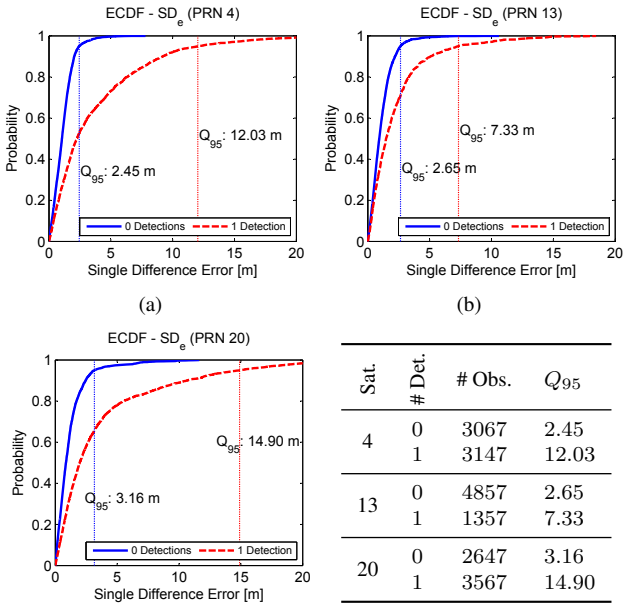

Sat.	# Det.	# Obs.	Q_{95}
4	0	3067	2.45
	1	3147	12.03
13	0	4857	2.65
	1	1357	7.33
20	0	2647	3.16
	1	3567	14.90

(d)

Figure 9. Measurement Domain Evaluation Results. (a)-(c) ECDF of single difference error for Satellites 4,13,20 (reference satellite:23). (d) Data summary

The choice of the reference satellite governs the precision of this estimate and should be made such that it is not affected by multipath, i.e. $m_\rho^{(\mathrm{ref})} \approx 0$. The probability for multipath reception correlates with the elevation angle of a satellite [5, Sec. 5.4.2]. A good choice for a reference satellite is therefore the one with the highest elevation angle.

The single difference error during the measurement period 1 is partitioned into two subsets based on whether or not multipath has been detected. An error analysis is performed for each partition.

Figures 9(a), 9(b), and 9(c) show the ECDF of the single difference error for Satellites 4, 13 and 20, respectively, indicating the 95th percentile Q_{95}. Figure 9(d) summarizes the underlying dataset. The results show the expected dependency of the multipath error on the satellite's elevation. Satellites 4 and 20 have similar elevations and hence similar error figures. On the contrary, signals from Satellite 13 experienced less detections and exhibit lower errors due to its higher elevation.

Figure 9 generally shows that our algorithm was able to identify a process of good measurements with a Q_{95} error of about 3 m and below. Moreover, it can be observed that false positive and false negative detections appeared. There are at least two reasons for this behavior. First, several assumptions and approximations are made which lead to minor errors. Second, even during multipath reception some error-free measurements occur because of a convenient combination of constructive and destructive interference.

Position Domain Evaluation

For the evaluation of the CMCD-based multipath detection performance in the position domain, the position of the

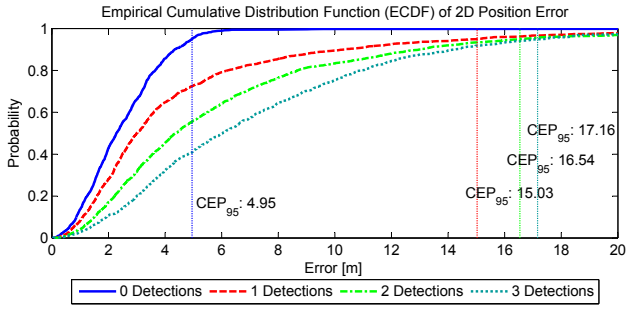

(a)

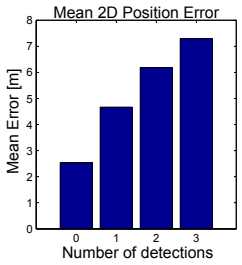

(b)

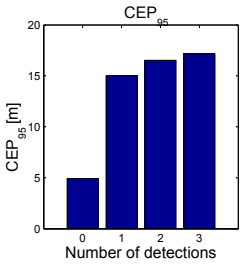

(c)

# Detections	# Observations	Mean	CEP_{95}
0	1332	2.53	4.95
1	2147	4.67	15.03
2	1972	6.19	16.54
3	702	7.29	17.16
(4)	(61)	(9.53)	(18.49)

(d)

Figure 10. (a) Single difference error, (b) Mean error per number of detections, (c) ECDF of 2D position error per number of detections, (d) CEP_{95} per number of detections, (e) Summary

receiver was calculated from the fixed set of Satellites 23, 20, 13 and 4. The horizontal (2D) position error was calculated with respect to the iTrace reference receiver. Data segments showing negligibly slow vehicle motion ($<$ 0.1 km/h) were disregarded from the analysis in order to assess the detection performance only at the correct mode of operation.

The set of position errors during motion was partitioned into cases where 0, 1, 2 or 3 detections occurred simultaneously. Each partition was then evaluated separately. Figure 10(a) shows the ECDF of the 2D position error for each data partition and indicates the 95th quantile (CEP_{95}). Figures 10(b) and 10(c) visualize the mean and the 95th quantile of the position error for each partition. Figure 10(d) summarizes the data and lists the corresponding number of observations in each partition.

CONCLUSION

In this work the concept of deltarange-based multipath detection with CMCD, a GNSS code multipath observable extending the idea of STDD, was derived. Further, a detection algorithm based on the statistical properties of CMCD was proposed. Two measurement campaigns were conducted to demonstrate the suitability of CMCD for mobile receivers in urban settings as well as to evaluate the algorithm's detection performance with real-world data.

First, fixed receiver measurements were shown to support the proposed model of zero-mean Gaussian distributed CMCD measurements in a no-multipath environment. The second measurement campaign employing a mobile receiver in an urban mutlipath scenario revealed a correlation between successful multipath detections and high errors in the measurement domain as well as position domain. Even though a rate of false positives can be observed in both evaluation methods, the ability to separate erroneous measurements from the measurement set has certainly been shown.

The visual inspection with the roof-mounted camera unveiled a considerable strength of CMCD-based multipath detection: Although the line-of-sight path to the majority of satellites was obstructed by tall buildings, the algorithm was still able to distinguish between mutlipath-corrupted and multipath-free satellite signals. This independence from measurement redundancy without the need for external data or state prediction is what sets CMCD or STDD apart from other approaches.

ACKNOWLEDGMENT

The authors would like to thank AUDI AG for their support during this project. Additionally, this work has been supported by the Computer Engineering and Networks Laboratory at ETH Zurich which is greatly appreciated.

REFERENCES

[1] H. K. Lee, J.-G. Lee, and G.-I. Jee, "GPS multipath detection based on sequence of successive-time double-differences," *Signal Processing Letters, IEEE*, vol. 11, no. 3, pp. 316–319, 2004.

[2] M. S. Braasch, "Multipath effects," *Global Positioning System Theory and Applications*, vol. 1, pp. 547–568, 1996.

[3] M. Irsigler, "Multipath propagation, mitigation and monitoring in the light of Galileo and the modernized GPS," *Ph. D. Thesis*, 2008.

[4] E. D. Kaplan and C. J. Hegarty, *Understanding GPS - Principles and Applications*. Artech House, 2005.

[5] P. Misra and P. Enge, *Global Positioning System: Signals, Measurements, and Performance*. Ganga-Jamuna Pr., 2011.

[6] R. D. Van Nee, "Multipath effects on gps code phase measurements," in *ION GPS-91; Proceedings of the 4th International Technical Meeting of the Institute of Navigation*, vol. 1, pp. 915–924, 1991.

[7] R. G. Brown, "Receiver autonomous integrity monitoring," *Global Positioning System: Theory and applications.*, vol. 2, pp. 143–165, 1996.

[8] L. Patino-Studencka, G. Rohmer, and J. Thielecke, "Approach for detection and identification of multiple faults in satellite navigation," in *Position Location and Navigation Symposium (PLANS), 2010 IEEE/ION*, pp. 221–226, 2010.

[9] T. Walter and P. Enge, "Weighted raim for precision approach," in *Proceedings of ION GPS*, vol. 8, pp. 1995–2004, 1995.

[10] P. J. G. Teunissen, "Quality control in integrated navigation systems," in *Position Location and Navigation Symposium*, pp. 158–165, IEEE, 1990.

[11] S. Hewitson and J. Wang, "Extended Receiver Autonomous Integrity Monitoring for GNSS/INS Integration," *Journal of Surveying Engineering*, vol. 136, no. 1, pp. 13–22, 2010.

[12] Y. Zhang and C. Bartone, "Multipath mitigation in the frequency domain," in *Position Location and Navigation Symposium, 2004. PLANS 2004*, pp. 486–495, April 2004.

[13] Q.-H. Phan, S.-L. Tan, and I. McLoughlin, "GPS multipath mitigation: a nonlinear regression approach," *GPS Solutions*, vol. 17, no. 3, pp. 371–380, 2013.

[14] M. Spangenberg, J.-Y. Tourneret, V. Calmettes, and G. Duchateau, "Detection of variance changes and mean value jumps in measurement noise for multipath mitigation in urban navigation," in *42nd Asilomar Conference on Signals, Systems and Computers*, pp. 1193–1197, 2008.

[15] S. Provost and A. Mathai, *Quadratic Forms in Random Variables: Theory and Applications*. Statistics: textbooks and monographs, CRC Press, 1992.